ELSEVIER

Signal Processing 80 (2000) 831–847

SIGNAL PROCESSING

www.elsevier.nl/locate/sigpro

Simple design of oversampled uniform DFT filter banks with applications to subband acoustic echo cancellation

Qing-Guang Liu[a], Benoît Champagne[b,*], Dominic K.C. Ho[c]

[a]*Sony Electronic Inc., Consumer AVD Engineering, 3300 Zanker Road, San Jose, CA 95134, USA*
[b]*Department of Electrical and Computer Engineering, McGill University, 3480 University Street, Montreal, Canada H3A 2A7*
[c]*Department of Electrical Engineering, University of Missouri-Columbia, Columbia, MO 65211, USA*

Received 10 December 1998; received in revised form 15 November 1999

Abstract

Subband adaptive filtering, which is the basis of modern acoustic echo cancellation (AEC) systems, is an important application of filter banks in which critical sampling cannot be used in general because of decimation aliasing effects. This leads to the use of oversampling schemes in the filter bank design wherein the perfect-reconstruction (PR) or near PR property is still required. In this work, a simple design technique for uniform DFT filter bank with near PR property is presented for the purpose of subband adaptive filtering. The prototype filter in the proposed filter banks is derived simply by performing an interpolation of a two-channel QMF filter, which can be obtained easily by computation or table look-up. An efficient implementation of the filter banks based on a weighted-overlap-add structure is described that allows flexibility in oversampling. The filter bank design technique presented in this paper is of particular interest in engineering applications, as demonstrated by design examples and experimental results in a real-time subband AEC application.

Zusammenfassung

Adaptive Filterung in Teilbändern, die die Basis moderner Systeme zur akustischen Echounterdrückung bilden, stellt eine wichtige Anwendung von Filterbänken dar, bei der eine Grenzabtastung im allgemeinen nicht vorgenommen werden kann, da es zu spektralen Überlappungseffekten durch Dezimation kommt. Daher werden Überabtastungsmethoden zum Filterbankentwurf benutzt, wobei die perfekte Rekonstruktions- (PR) oder beinahe-PR Eigenschaft erhalten bleiben muß. In dieser Arbeit wird ein einfaches Entwurfsverfahren für einheitliche DFT Filterbänke vorgestellt, die beinahe-PR Eigenschaften besitzen, und die zur adaptiven Filterung in Teilbändern bestimmt sind. Das Prototypfilter für die vorgeschlagene Filterbank wird einfach durch Interpolation eines zweikanaligen QMF Filters gewonnen, welches sich durch einfache Berechnungen oder Tabellensuche bestimmen läßt. Anschließend wird cine effiziente, auf einer gewichteten overlap-add Methode basierende Implementierung der Filterbänke beschrieben, die hinsichtlich der Überabtastung Flexibilität erlaubt. Die in diesem Artikel vorgestellte Filterbankentwurfsmethode ist in Ingenieuranwendungen von besonderem Interesse, wie anhand von Entwurfsbeispielen und Ergebnissen von Experimenten gezeigt wird, die zur akustischen Echounterdrückung in Teilbändern und unter Echtzeitbedingungen durchgeführt wurden.

* Corresponding author. Tel.: +1-514-398-5701; fax: +1-514-398-4470.
E-mail address: champagne@ece.mcgill.ca (B. Champagne)

0165-1684/00/$ - see front matter
PII: S0165-1684(99)00165-6

Nomenclature

α	a weighting factor	L	length of analysis filter $h(n)$ ($L = IL_0$)
$A_k(z)$	aliasing component in kth subband	L_0	length of 2-channel QMF prototype $h_0(n)$ (even)
$A(\omega)$	measure of subband decimation aliasing	m	discrete-time index at low sampling rate (after decimation)
E	error function used in filter design	M	downsampling factor
E_s	stop-band energy	n	discrete-time index at high sampling rate
E_r	amplitude distorsion	$T_k(z)$	input–output transfer function for kth aliasing component
$E(\omega)$	measure of full-band aliasing distorsion	$\tilde{T}_0(z)$	input–output transfer function of 2-channel QMF bank
$E_k(m)$	kth subband residual signal in AEC experiments	$x(n)$	input of analysis bank; loudspeaker signal in AEC experiments
$F(z)$	anti-imaging low-pass filter	$\hat{x}(n)$	output of synthesis bank
F_s	original sampling rate	$X_k(z)$	z-transform of kth subband signal
F'_s	sampling rate after downsampling	$\hat{X}(z)$	z-transform of $\hat{x}(n)$
$g(n)$	impulse response of synthesis filter	$y(n)$	microphone signal in AEC experiments
$G(z)$	z-transform of $g(n)$	W_K, W_M	phase factors
$h(n)$	impulse response of analysis filter	ω	angular frequency
$h_0(n)$	impulse response of 2-channel QMF prototype	ω_c	cutoff frequency of analysis filter
$H(z)$	z-transform of $h(n)$		
k, l	subband indices		
K	number of subbands (even)		
I	interpolation factor ($I = K/2$)		

Résumé

Le filtrage adaptatif en sous-bandes, qui est à la base des plus récents systèmes d'annulation d'écho acoustique, est une application importante des bancs de filtres dans laquelle l'échantillonage critique ne peut être utilisé en raison des effets d'emprunt résultant de la décimation. Cela conduit à l'utilisation du sur-échantillonnage dans la conception des bancs de filtres, où des propriétés de reconstruction parfaite (PR) ou presque parfaite (NPR) sont toujours requises. Dans cet article, nous présentons une technique de conception simple pour des bancs de filtres de type DFT-uniforme avec propriété NPR, pour les applications de filtrage adaptatif en sous-bandes. Le filtre prototype dans les bancs de filtres proposés est calculé simplement par interpolation d'un filtre QMF à deux canaux, ce dernier pouvant être obtenu par optimization non-linéaire ou trivialement par lecture d'une table. Une mise en oeuvre efficace des bancs de filtres proposés, reposant sur la structure WOA et permettant l'utilisation d'un facteur de décimation arbitraire, est décrite. La technique de conception de banc de filtres présentée dans cet article revêt un intérêt particulier pour les applications en génie, tel que démontré par des exemples de conception et les résultats expérimentaux d'une application de AEC en sous-bandes sur un processeur à temps réel.

Keywords: Oversampled filter banks; Uniform DFT filter banks; Multi-rate signal processing; Filter design; Subband adaptive filtering; Acoustic echo cancellation

1. Introduction

Multirate filter banks have been a subject of considerable interest in the field of digital signal processing for many years [3,17,18]. One typical application of filter banks is in subband coding, where each subband is maximally decimated and the perfect-reconstruction (PR) or near PR property is required for the analysis and synthesis banks [17,18]. Another important application of filter banks is in subband adaptive filtering, which has received much attention in recent years especially in the context of acoustic echo cancellation (AEC) [7,11].

In a typical subband filtering scheme for AEC, both the input (loudspeaker) and reference (microphone) signals are split into subbands by analysis banks. Adaptive filters are applied in each subband at a decimated rate and the subband residuals (i.e. after echo removal) are recombined by a synthesis bank to create a full-band output signal at the original rate. Since the reference signal may contain a local speech component that will go through the cascade of an analysis and a synthesis bank prior to its transmission, a near-PR property is needed for the filter banks.

Compared with the full-band case, subband adaptive filtering achieves a gain in computational complexity as a result of sampling rate reduction of the subband signals. However, due to aliasing effects in the analysis bank, critically sampled (i.e. maximally decimated) filter banks, which have received considerable attention in the literature and are used in subband coding, cannot be applied directly in a subband system for AEC [8]. Accordingly, an oversampling scheme (i.e. non-critical sampling) is often used in subband to keep aliasing distortion in the full-band output of the synthesis bank below an acceptable level. Thus, only amplitude and phase distortions need to be taken into account in the PR filter bank design, which leads to a relatively simpler design problem than in the critically sampled case. In AEC application, only a near-PR property is required for the filter bank, so that the design constraints are further relaxed.

General criteria for designing oversampled filter banks have been described earlier in [3] and some more recent theoretical advances on PR oversampled filter banks can be found in [4,12,14]. Some basic considerations regarding the use of oversampling filter banks in subband AEC applications are given in [6,11], while specific structures and/or designs are reported in [1,5,9,15]. In [15], oversampled quadrature mirror filter (QMF) banks are proposed that avoid subband aliasing by limiting the downsampling factor to be exactly one half of the number of subbands. In [1], a Weaver SSB subband structure is described but the downsampling factor is limited in the same way. In [5], a method is proposed for the design of non-symmetrical (i.e. increased analysis bandwidth) oversampled filter banks with low processing delays, based on non-linear phase M-band prototype filters optimized via a constrained eigenfilter approach. Low delay is generally achieved at the cost of increasing the length of the prototype filter; the issue of efficient implementation is not addressed. In [9], the use of a non-uniform subband structure with different down-sampling rates in adjacent subbands is suggested to minimize aliasing effects; a modified eigenfilter approach is also used for the prototype design.

Despite these recent advances, there remains a strong need to provide DSP engineers with simple and concrete methods for the rapid design and prototyping of filter banks suitable for subband AEC applications. In this respect, particularly important design requirements include the possibility of arbitrary oversampling in decimation, near-PR property of the combined analysis/synthesis banks, low complexity of implementation and low processing delay.

In this paper, motived by the above considerations, we present a simple and systematic design technique for uniform DFT filter banks, which satisfy near-PR property in the oversampling scheme. With the proposed filter bank structure, design of the analysis/synthesis prototype filter simply amounts to performing an interpolation of the well-known two-channel quadrature mirror filters (QMF), which have been tabulated in [3,10]. A weighted-overlap-add (WOA) approach [3] is described for the specific implementation of the filter banks such that an arbitrary sampling rate in subbands can be obtained efficiently. The effectiveness of the proposed methodology in

engineering applications is demonstrated by means of filter bank design examples and experimental results of a real-time subband AEC system developed around one of these examples.

The paper is organized as follows. In Section 2, the structure of the modified uniform DFT filter banks that we propose is presented and its properties are analyzed. In Section 3, we provide a simple approach for the prototype filter design, while the efficient realization of the filter banks based on the WOA method is described in Section 4. Design examples and experimental results of a real-time subband AEC system are presented in Section 5. Some concluding remarks are provided in Section 6.

2. A structure for uniform DFT filter banks

A structural diagram of the proposed K-channel uniform DFT filter banks is shown in Fig. 1. In the analysis bank, a complex modulation function W_K^{-kn}, where $W_K = \exp(\mathrm{j}2\pi/K)$, $k = 0, \ldots, K-1$ is the channel index and n is the discrete-time index at high sampling rate, is applied to the input signal $x(n)$. The analysis filter, represented by its impulse response $h(n)$, is a low-pass filter with cutoff frequency $\omega_c = \pi/K$. Let $H(z) = \sum_{n=-\infty}^{\infty} h(n)z^{-n}$ denote the z-transform of $h(n)$. The ideal low-pass

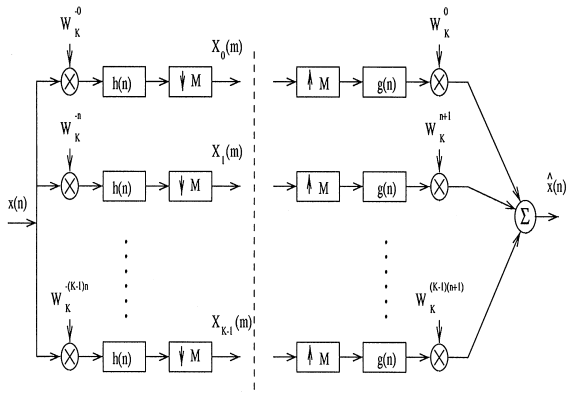

Fig. 1. Uniform DFT filter banks: analyzer (left) and synthesizer (right).

property for $H(z)$ should be

$$|H_{\mathrm{ideal}}(\mathrm{e}^{\mathrm{j}\omega})| = \begin{cases} 1, & 0 \leqslant |\omega| \leqslant \omega_c, \\ 0, & \omega_c < |\omega| \leqslant \pi. \end{cases} \tag{1}$$

After modulation and low-pass filtering, the signal in the kth branch is decimated by an integer factor M to produce the desired subband signal, $X_k(m)$, where m is the discrete-time index at low sampling rate. The latter can be expressed in the z-domain as

$$X_k(z) = \frac{1}{M}\sum_{l=0}^{M-1} H(z^{1/M}W_M^{-l})X(z^{1/M}W_M^{-l}W_K^k), \tag{2}$$

where $W_M = \exp(\mathrm{j}2\pi/M)$. For subsequent discussions, it is convenient to rewrite (2) in the form

$$X_k(z) = \frac{1}{M}H(z^{1/M})X(z^{1/M}W_K^k) + A_k(z), \tag{3}$$

where

$$A_k(z) = \frac{1}{M}\sum_{l=1}^{M-1} H(z^{1/M}W_M^{-l})X(z^{1/M}W_M^{-l}W_K^k) \tag{4}$$

is viewed as the aliasing component due to decimation in the kth subband signal $X_k(z)$. In the application of subband adaptive filtering to AEC, this kind of frequency-domain aliasing must be avoided to achieve effective cancellation of acoustic echoes [7,8]. Note that the aliasing component $A_k(z)$ is affected by the stop-band property of the low-pass filter $H(\mathrm{e}^{\mathrm{j}\omega})$. Since the ideal low-pass characteristic (1) can only be approximated in practice, i.e. in the case of a realizable (i.e. causal and stable) filter $H(\mathrm{e}^{\mathrm{j}\omega})$, a transition band does exist for $H(\mathrm{e}^{\mathrm{j}\omega})$ and significant aliasing components will generally be created if the critical downsampling factor $M = K$ is used in the subbands. Thus, an oversampling scheme, i.e., $M < K$, is often used in filter banks for subband adaptive filtering. In this work, we assume that $M < K$, such that frequency-domain aliasing can be made acceptably small.

In the synthesis bank shown in Fig. 1, each subband signal is first upsampled by the factor M and then passed to a common synthesis filter $g(n)$, or equivalently $G(z)$, which is also a low-pass filter with cutoff frequency $\omega_c = \pi/K$. The outputs

from each filter are demodulated and then added to produce the synthesized output $\hat{x}(n)$. We note that the proposed analysis/synthesis filter bank pair in Fig. 1 differs from the generalized DFT (GDFT) analysis/synthesis pair [3] in that the modulation function in the synthesis bank is not the complex conjugate of the modulation function in the analysis bank; it is rather given by $W_K^{k(n+1)}$, $k = 0, \ldots, K-1$. With such a modulation function in the synthesis bank, the phase distortion in its full-band output $\hat{x}(n)$ can be conveniently eliminated, as will be demonstrated below.

If no modifications are made to the subband signals $X_k(z)$, the synthesizer output $\hat{x}(n)$ can be expressed in the z-domain as

$$\hat{X}(z) = \sum_{k=0}^{K-1} X_k(z^M W_K^{-kM}) G(zW_K^{-k}) W_K^k. \tag{5}$$

Substituting (2) into (5), we have

$$\hat{X}(z) = \sum_{l=0}^{M-1} T_l(z) X(zW_M^{-l}), \tag{6}$$

where

$$T_l(z) = \frac{1}{M} \sum_{k=0}^{K-1} W_K^k H(zW_K^{-k} W_M^{-l}) G(zW_K^{-k}). \tag{7}$$

Since the filters $H(z)$ and $G(z)$ are both low pass with the same cutoff frequency $\omega_c = \pi/K$, under the assumption $M < K$, the pass-band of $G(zW_K^{-k})$ will fall well into the stop band of $H(zW_K^{-k}W_M^{-l})$ for $l = 1, \ldots, M-1$, and vice versa. As a result, the term $H(zW_K^{-k}W_M^{-l})G(zW_K^{-k})$ on the right-hand side of (7) can be neglected, i.e. $T_l(z) \approx 0$, for $l = 1, \ldots, M-1$. Thus, the aliasing components in (6) are approximately eliminated and the latter reduces to

$$\hat{X}(z) \approx T_0(z) X(z), \tag{8}$$

where

$$T_0(z) = \frac{1}{M} \sum_{k=0}^{K-1} W_K^k H(zW_K^{-k}) G(zW_K^{-k}). \tag{9}$$

We emphasize the facts that (8) is an approximation and that in practice, a certain aliasing error will be present in the reconstructed output of the filter banks. This issue if given additional consideration in Section 5.

According to (8) $T_0(z)$ can be regarded as the overall transfer function of the cascade of the analysis and the synthesis banks, i.e., from $X(z)$ to $\hat{X}(z)$. For a PR system, the reconstructed signal $\hat{x}(n)$ must be an exact replica of $x(n)$, except possibly for a constant time delay and a scalar. To achieve this effect, the phase of $T_0(e^{j\omega})$ should thus be linear (i.e., eliminating phase distortion) and the amplitude $|T_0(e^{j\omega})|$ should be constant (i.e., eliminating amplitude distortion). At first, we show how to eliminate phase distortion.

Let the analysis filter $h(n)$ be a finite impulse response (FIR) filter with length L (i.e., $h(n) = 0$ for $n < 0$ and $n \geqslant L$). Then, $H(z)$ can be expressed as

$$H(z) = \sum_{n=0}^{L-1} h(n) z^{-n}. \tag{10}$$

Let the synthesis filter $g(n)$ be obtained by flipping (i.e, time reversal of) $h(n)$ in the time domain, that is

$$g(n) = h(L-n-1), \quad n = 0, \ldots, L-1. \tag{11}$$

If $h(n)$ is symmetrical with respect to the middle point $(L-1)/2$, as is the case for a low-pass linear phase filter, $g(n)$ will be identical to $h(n)$. In the z-domain, corresponding to (11), we have

$$G(z) = z^{-(L-1)} H(z^{-1}). \tag{12}$$

Substituting (12) into (9), one obtains

$$T_0(z) = z^{-(L-1)} \frac{1}{M} \sum_{k=0}^{K-1} W_K^{kL} H(zW_K^{-k}) H(z^{-1}W_K^k). \tag{13}$$

Assume now that the filter length L can be expressed as a multiple of the subband number K, i.e., $L = \rho K$, where ρ is an integer. Then in the frequency domain, (13) becomes

$$T_0(e^{j\omega}) = e^{-j(L-1)\omega} \frac{1}{M} \sum_{k=0}^{K-1} |H(e^{j\omega} W_K^{-k})|^2. \tag{14}$$

Clearly, $T_0(e^{j\omega})$ has a linear phase, which is the desired result.

Here, the phase distortion is completely eliminated by choosing $g(n)$ as in (11). Then, it remains only to eliminate the amplitude distortion. According to (14), an ideal flatness requirement for $|T_0(e^{j\omega})|$ can now be expressed as

$$\sum_{k=0}^{K-1} |H(e^{j\omega} W_K^{-k})|^2 = 1 \quad \text{for all } \omega; \tag{15}$$

which is a power complementarity condition. In the next section, a simple approach is given to design the prototype filter $H(z)$ such that $|T_0(e^{j\omega})|$ is acceptably flat.

3. Prototype filter design

Ideally, the prototype filter requirements for the problem at hand can be summarized by (1) and (15). Since (1) cannot be satisfied exactly for any FIR filter $H(z)$, the design problem thus converts to approximate these requirements under a certain criterion. A commonly used criterion [10,17] is to minimize an error function E, which is defined as

$$E = \alpha E_s + E_r, \tag{16}$$

where α is a real positive weighting factor while E_s and E_r express the errors in approximating conditions (1) and (15), and are, respectively, given by

$$E_s = \int_{\omega_s}^{\pi} |H(e^{j\omega})|^2 \, d\omega, \tag{17}$$

$$E_r = \int_0^{2\pi} \left(\sum_{k=0}^{K-1} |H(e^{j\omega} W_K^{-k})|^2 - 1 \right)^2 d\omega. \tag{18}$$

In (17), ω_s ($\omega_s > \omega_c$) is the stopband edge which determines the transition band of $H(e^{j\omega})$. The basic idea of the technique that we propose below for the design of the prototype $h(n)$ is to transform the K-channel problem (16)–(18) into an equivalent problem for a two-channel QMF bank. Solutions for the latter can then be obtained easily by computation or "table look-up". The details of this approach are now exposed.

Suppose K is even, i.e., $K = 2I$, where I is positive integer. When $K = 2$ (i.e., $I = 1$) and $h(n)$ is symmetrical, the cost function in (16) is identical to that used in Johnston's scheme [10]. As a result, minimizing (16) will lead to solutions for the well-known two-channel QMF bank. Let $h_0(n)$ denote the resulting QMF prototype. The corresponding transfer function $\tilde{T}_0(e^{j\omega})$, obtained from (14) with $K = 2$, will be

$$\tilde{T}_0(e^{j\omega}) = e^{-j(L-1)\omega} \tfrac{1}{2} \{ |H_0(e^{j\omega})|^2 + |H_0(-e^{j\omega})|^2 \}. \tag{19}$$

We recall that QMF filters have been widely used in two-channel filter banks and their coefficients have been tabulated in [10,3] for various choices of the parameters L,α and ω_s.

For $I > 1$, solutions for the filter design based on minimizing the cost function (16) can be obtained with the use of computer-aided optimization techniques. For example, the Hooke and Jeaves search algorithm used in Johnston's scheme [10] can also be applied to (16) for designing $h(n)$. Instead of using complex optimization programs, however, we will show that a simple way to design $h(n)$ is just to perform an I-point interpolation of a two-channel QMF prototype $h_0(n)$. The simplicity of this design procedure will bring great convenience in practical engineering applications.

To this end, let $h(n)$ be obtained from the I-point interpolation of $h_0(n)$, i.e., upsampling by I followed by anti-imaging low-pass filtering. The resulting frequency response is

$$H(e^{j\omega}) = H_0(e^{jI\omega}) F(e^{j\omega}), \tag{20}$$

where $F(e^{j\omega})$ is a low-pass filter with cutoff frequency at π/I. The amplitude responses for $H_0(e^{jI\omega})$ and $F(e^{j\omega})$ are illustrated in Fig. 2. Since $H_0(e^{j\omega})$ itself is low pass with cutoff frequency at $\pi/2$, it is not difficult to design the anti-imaging filter $F(e^{j\omega})$ such that (see Fig. 2)

$$|H(e^{j\omega})| = |H_0(e^{jI\omega}) F(e^{j\omega})| = \begin{cases} |H_0(e^{jI\omega}), & |\omega| \leqslant \frac{\pi}{I}, \\ 0, & \frac{\pi}{I} < |\omega| < \pi. \end{cases} \tag{21}$$

A simple way to perform such an I-point interpolation, for example, is to use the Matlab interpolation

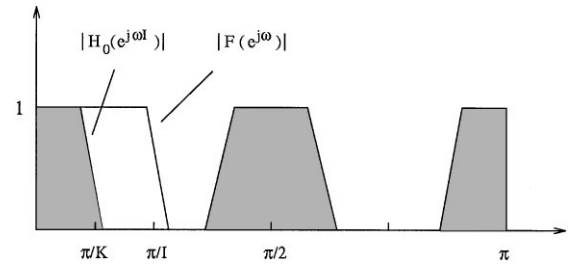

Fig. 2. Amplitude responses of $H_0(e^{j\omega I})$ and $F(e^{j\omega})$ (here $K = 8$).

function interp(). Specifically, the command h = interp(h0,I), where the vectors h and h0, respectively, contain the coefficients of the desired prototype $h(n)$ and the two-channel QMF prototype $h_0(n)$, will result in $h(n)$ satisfying the property (21) with a good approximation. Note that according to our previous notations, the length of the two-channel QMF prototype $h_0(n)$ must be specified as $L_0 = 2\rho$, so that the length of the prototype $h(n)$ resulting from the interpolation is $2\rho I = K\rho = L$, as desired for the linear-phase property of $T_0(z)$ (14).

Replacing ω by $\omega - 2\pi k/K$ in (21) and recalling that $H(e^{j\omega})$ is periodic with period 2π, we obtain the following expressions:

$$|H(e^{j\omega}W_K^{-k})| = \begin{cases} |H_0(e^{j(\omega I - k\pi)})|, & (k-1)\frac{\pi}{I} \leqslant \omega \leqslant (k+1)\frac{\pi}{I}, \\ 0, & \text{otherwise} \end{cases} \quad (22)$$

for $k = 0, \ldots, K-1$. Based on (22), we note that whenever ω belongs to the interval $(l\pi/I, (l+1)\pi/I]$ for some $l \in \{0, \ldots, K-1\}$, only the two terms with $k = l$ and $l+1$ give a non-zero contribution in the right-hand side of (14). That is,

$$T_0(e^{j\omega}) = e^{-j(L-1)\omega}\frac{1}{M}\{|H_0(e^{j(\omega I - l\pi)})|^2 + |H_0(e^{j(\omega I - (l+1)\pi)})|^2\}$$

$$\text{for } l\frac{\pi}{I} < \omega \leqslant (l+1)\frac{\pi}{I}, \quad l = 0, \ldots, K-1. \quad (23)$$

Now, considering (23) over the complete frequency interval and recalling that $e^{jl\pi} = \pm 1$, we easily obtain

$$T_0(e^{j\omega}) = e^{-j(L-1)\omega}\frac{1}{M}\{|H_0(e^{j(\omega I)})|^2 + |H_0(-e^{j(\omega I)})|^2\}. \quad (24)$$

Comparing (24) with (19), we see that $|T_0(e^{j\omega})|$ has the same flatness as $|\tilde{T}_0(e^{j\omega})|$. Thus, the reconstruction error for the filter bank with $H(e^{j\omega})$ should be consistent with that for the corresponding two-channel QMF bank based on the $K = 2$ prototype $h_0(n)$. In practical filter design, the former might slightly exceed the latter because the property in Eq. (21) cannot be met exactly. This difference, however, can usually be neglected in practice.

In summary, the prototype filter $h(n)$ used for the K-channel filter bank in Fig. 1 can be obtained by performing a $K/2$-point interpolation on a two-channel QMF prototype $h_0(n)$. The reconstruction error is determined by the corresponding two-channel QMF bank. As mentioned earlier, QMF prototypes can be found conveniently from tables in [10,3] and a Matlab interpolation function can be used to perform the corresponding interpolation. In this way, the usual filter design procedure which needs complex optimization programming is avoided. This characteristic is of particular significance in engineering applications.

As a final note, observe that if the QMF prototype $h_0(n)$ is originally scaled so that $|H_0(e^{j\omega})|^2 + |H_0(-e^{j\omega})|^2 \approx 1$, then from (24), we have $|T_0(e^{j\omega})| \approx 1/M$. According to (8), this implies that the uniform DFT filter bank will introduce a gain of $1/M$. Thus, if a transmission gain of unity is desired, amplification by a factor M must be provided along the signal path from input to output.

4. Efficient WOA realization

It is well known that the uniform DFT filter bank is the most efficient one in terms of realization. There are basically two different approaches for the efficient realization of uniform DFT filter banks [3]: one is based on the polyphase structure and the other one is based on the weighted-overlap-add (WOA) structure. The polyphase structure

is suitable for a decimation factor M satisfying $K = Mi$, where i is a positive integer. The WOA structure is more general and can be used easily with arbitrary values of the decimation factor M. In the context of subband adaptive filtering and especially AEC, the WOA structure is thus preferred since it offers more flexibility in the selection of the decimation factor M. Referring to Fig. 1, the WOA method for the realization of the uniform DFT analysis bank can be found in [3]; accordingly, only the WOA realization of the synthesis bank is described in this section.

Since the synthesis bank in Fig. 1 differs from the conventional uniform DFT synthesis bank [3] in the choice of the demodulation function, corresponding differences will appear in their WOA-based realizations. A block diagram for implementing the WOA structure of the modified synthesis bank that we propose in Fig. 1 can be obtained from an investigation of expression (5); it is shown in Fig. 3. The corresponding implementation steps are summarized below:

1. At time m (lower sampling rate), apply a K-point discrete Fourier transform (DFT) to the set of complex conjugate subband signal samples $\hat{X}_k^*(m)$, $k = 0, \ldots, K-1$. Let $\hat{x}_m(r)$, $r = 0, \ldots, K-1$, denote the resulting output.
2. Apply a modulo-K shift by $-mM$ samples to the sequence $\hat{x}_m(r)$, $r = 0, \ldots, K-1$: the result of this operation is represented by $\hat{\xi}_m(r) = \hat{x}_m((r + mM) \text{ modulo } K)$, $r = 0, \ldots, K-1$.
3. Periodically extend $\hat{\xi}_m(r)$, $r = 0, \ldots, K-1$, into a sequence of L samples (the length of the prototype filter). To simplify the notation, we denote the periodically extended signal by $\hat{\xi}_m(r)$ but now the index r runs from $r = 0$ to $r = L-1$.

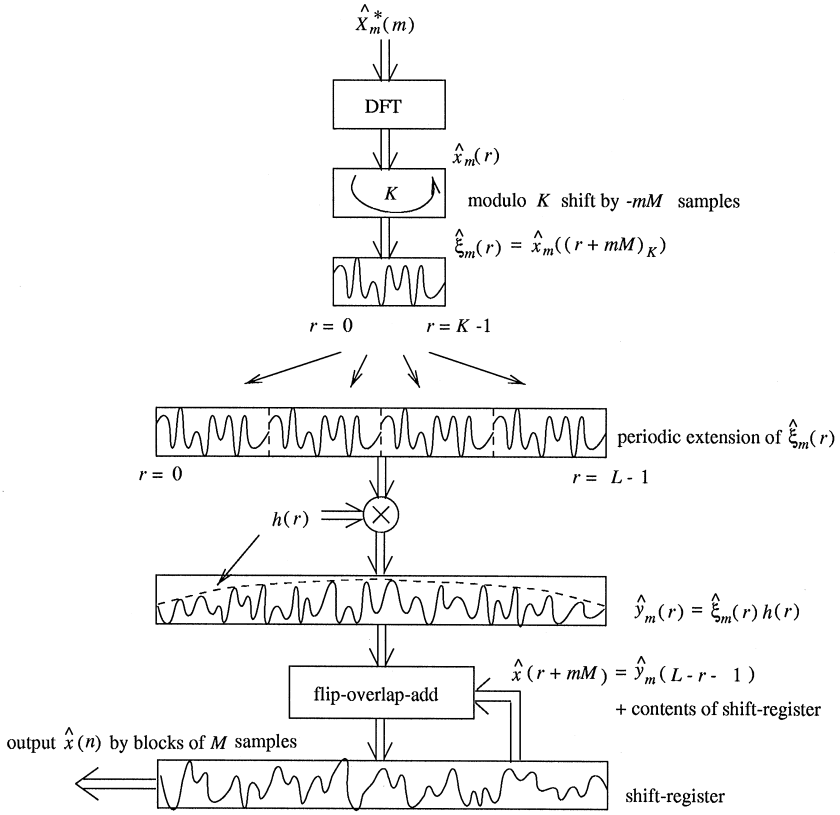

Fig. 3. Implementation of the synthesis bank by using the weighted overlap-add approach.

4. Perform sample-by-sample multiplication of the periodically extended signal $\hat{\tilde{\xi}}_m(r)$ with the analysis filter $h(n)$: that is, compute $\hat{y}_m(r) = \hat{\tilde{\xi}}_m(r)h(r)$, $r = 0, \ldots, L-1$.
5. Perform a flip-overlap-add operation on $\hat{y}_m(r)$. More specifically, this operation uses an output-signal shift register of length L whose samples are indexed with $r = 0, \ldots, L-1$. At the beginning of operations, this register is initialized to zero. To obtain the full-band signal samples corresponding to the subband samples $\hat{X}_k(m)$ at time m (lower sampling rate), the following operations are proposed:
   (a) flip the sequence $\hat{y}_m(r)$ into $\hat{y}_m(L-1-r)$, $r = 0, \ldots, L-1$.
   (b) overlap-and-add the flipped sequence to the previous content of the shift-register, sample by sample.
6. Following these operations, the first M samples of the output buffer, which is represented in Fig. 3 by $\hat{x}(mM + r)$, $r = 0, \ldots, L-1$, correspond to the desired output signal samples. Thus, the last step consists in shifting the output buffer to the left by M samples and reading the desired block of M output samples.

To construct the complete sequence of synthesized samples $\hat{x}(n)$, $n = 0,1,2, \ldots$, the above sequence of operations is repeated every M samples.

If the fast Fourier transform (FFT) is used for the realization of the DFT, the computational requirements for the above WOA realization of the synthesis bank is $L + K \log_2 K$ real multiplications per M input (output) samples. The computational complexity of the WOA realization of the analysis bank is identical [3].

5. Design examples and application

In this section, the engineering effectiveness of the proposed design methodology for uniform DFT filter banks is demonstrated in two different ways: (i) design examples of modified uniform DFT filter banks; (ii) experimental results of a subband AEC system developed around one of these design examples

5.1. Design examples

To evaluate the near-PR property of a subband system, three kinds of distortion need to be investigated, namely: aliasing, amplitude and phase distortions. Since the phase distortion is exactly eliminated in the proposed filter banks, only the other two kinds of distortion need to be considered. The amplitude distortion can be measured from the peak ripple of $M|T_0(e^{j\omega})|$, where $T_0(e^{j\omega})$ is defined in (24), while a measure for evaluating the full-band aliasing distortion is given by [13,17]

$$E(\omega) = \sqrt{\sum_{l=1}^{M-1} |T_l(e^{j\omega})|^2}, \quad |\omega| \leqslant \pi, \tag{25}$$

where $|T_l(e^{j\omega})|$, $l = 1, \ldots, M-1$, can be obtained from (7). The maximum value of $E(\omega)$ over all ω is called *peak aliasing distortion*.

Besides the PR property of the overall subband system, we also need to investigate the decimation aliasing components within the subbands since subband adaptive filtering could be seriously affected by such aliasing, as we mentioned earlier. The decimation aliasing component in the kth subband is given by $A_k(z)$ in (4). Similarly to the definition for the aliasing distortion in (25), a decimation aliasing function based on (4) is defined as follows:

$$A(\omega) = \sqrt{\sum_{l=1}^{M-1} |H(e^{j\omega/M} W_M^{-l})|^2} \quad \text{for } |\omega| \leqslant \pi. \tag{26}$$

The function $A(\omega)$ so defined is independent of the subband index k. Note that the absence of the full-band aliasing distortion (i.e., $E(\omega) = 0$) does not mean that there is no decimation aliasing in the subbands; however, if there is aliasing distortion in the full band, there must be decimation aliasing in subbands.

Design Example 1. In this example, we consider the QMF filter 32D tabulated in [3,10], as the selected choice for $h_0(n)$. This filter has a total of $L_0 = 32$ symmetrical coefficients and its stop-band attenuation is 38 dB; when used in a two-channel QMF bank, the reconstruction error is 0.025 dB. To design a $K = 8$ channel filter bank, $h(n)$ is obtained from $h_0(n)$ by using the Matlab function

`h = interp(h0,4)` (i.e. interpolation by $I = 4$). The resulting prototype filter $h(n)$ has $L = 128$ coefficients. Fig. 4 shows the magnitude response of $H(\omega)$; its (normalized) cut-off frequency of is $0.5/8 = 0.0625$.

The amplitude distortion of the filter bank, which can be seen from the plot of $M|T_0(e^{j\omega})|$ in Fig. 5, is within $\pm$ 0.04 dB. The decimation aliasing function $A(\omega)$ (26) and the full-band aliasing distortion $E(\omega)$ (25) are plotted in Figs. 6 and 7, respectively, for different values of the downsampling factor M. For critical downsampling, i.e. $M = 8$, the plot of $A(\omega)$ in Fig. 6 reveals the presence of large aliasing components at high frequency in each subband. This results in large aliasing errors around the boundary of each subband in the full-band output, as can be seen from the corresponding plot of $E(\omega)$ in Fig. 7. Based on Figs. 6 and 7, we see that both decimation aliasing in subbands and aliasing errors in the full-band are acceptably small when $M \leqslant 7$. Thus, in this example, filter banks which can be used appropriately for subband adaptive filtering can be obtained by choosing $M = 7$ in the designed filter banks.

Design Example 2. In the second example, a $K = 16$ channel filter bank is designed by using the proposed approach. In order for the prototype filter $h(n)$ to have the same length as in Example 1, i.e., $L = 128$, $h(n)$ is now obtained via an $I = 8$ point interpolation of the QMF filter 16 A from [10,3], which consists of $L_0 = 16$ coefficients. Again, the Matlab function `interp(,)` is used for this purpose. The amplitude response of the resulting prototype filter $h(n)$ is shown in Fig. 8.

The amplitude distortion function $M|T_0(e^{j\omega})|$ is plotted in Fig. 9; it remains within $\pm$ 0.05 dB. The decimation aliasing function $A(\omega)$ for different values of M is shown in Fig. 10. We see that the decimation aliasing becomes significant for smaller ratios of M/K when compared to Example 1. This is because the frequency property of the prototype filter shown in Fig. 8 is not as good as that shown in Fig. 4, as a result of the reduced bandwidth. The aliasing error $E(\omega)$ for several values of M is shown in Fig. 11, while the peak aliasing distortion is plotted in Fig. 12 as a function of M. In this example, a proper choice of M for the application of subband adaptive filtering should be $M = 12$ or 13.

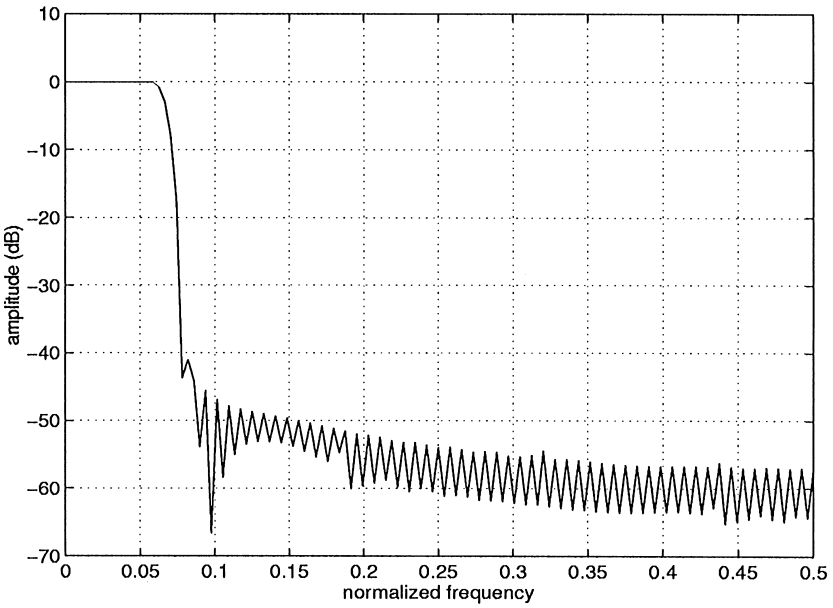

Fig. 4. Example 1: magnitude response of a $K = 8$ channel prototype filter with length $L = 128$.

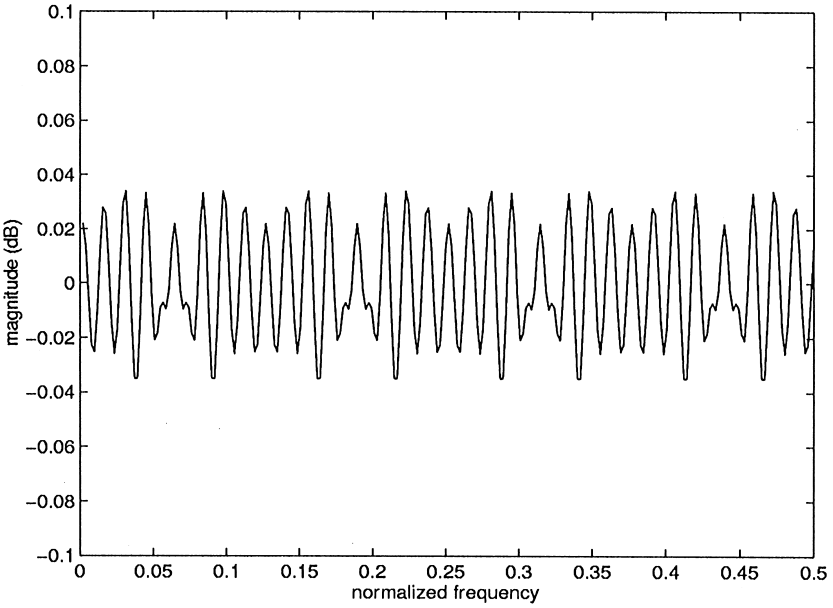

Fig. 5. Example 1: magnitude distortion $M|T_0(e^{j\omega})|$.

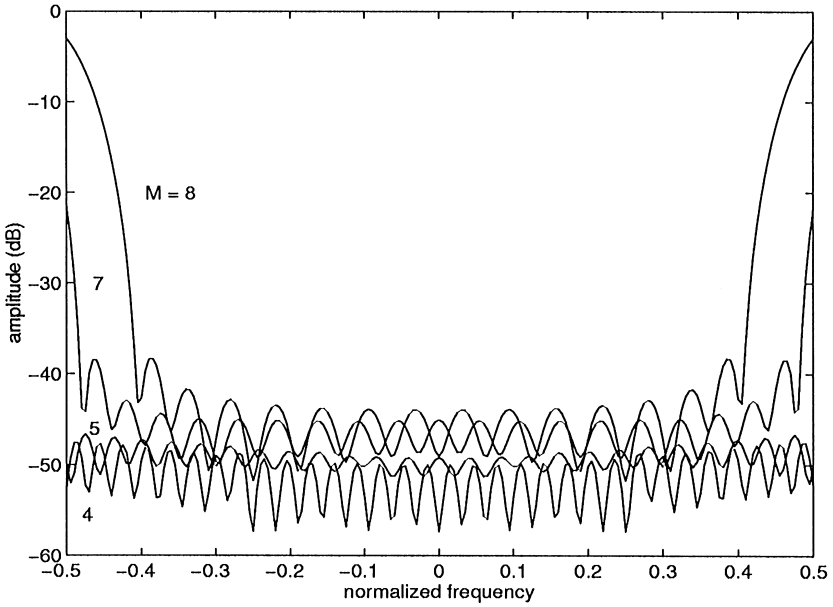

Fig. 6. Example 1: decimation aliasing $A(\omega)$ in subbands for different values of downsampling factor M.

5.2. Subband AEC application

To evaluate the practical merit of the proposed design method in AEC applications, a subband AEC system based on filter bank design Example 2 was implemented in real time on a floating-point processor and evaluated under normal operating conditions. We briefly describe this system and

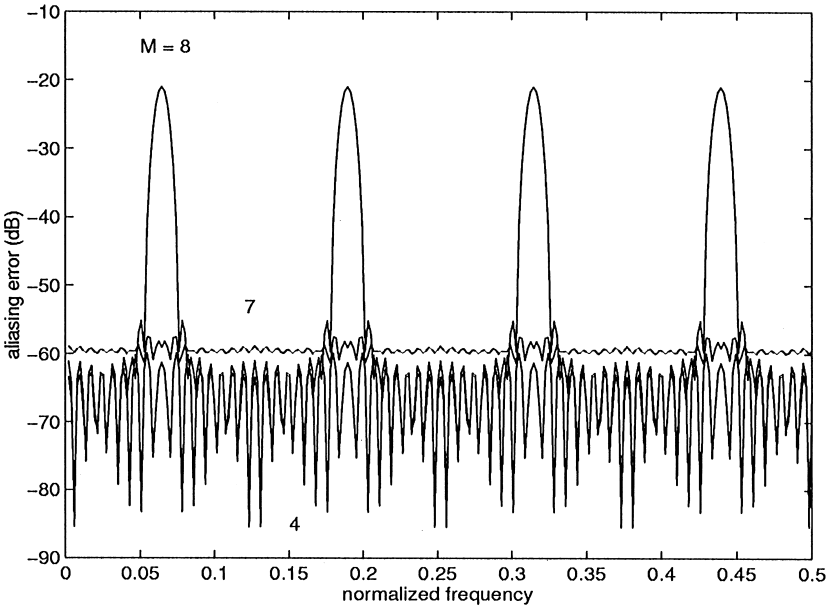

Fig. 7. Example 1: aliasing distortion $E(\omega)$ of the filter banks for different downsampling factors M.

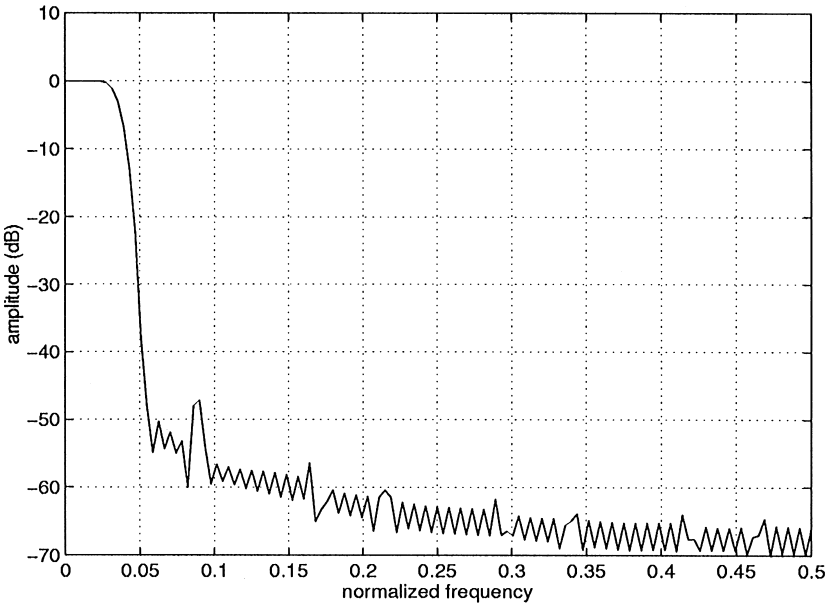

Fig. 8. Example 2: magnitude response of a $K = 16$ channel prototype filter with length $L = 128$.

provide experimental results that demonstrate the effectiveness of the proposed approach.

The structure of the subband AEC system is illustrated in Fig. 13. It consists of two analysis filter banks, a synthesis bank and a set of subband adaptive filters. The analysis banks are used to split the loudspeaker and microphone signals, respectively, $x(n)$ and $y(n)$ originally sampled at the rate

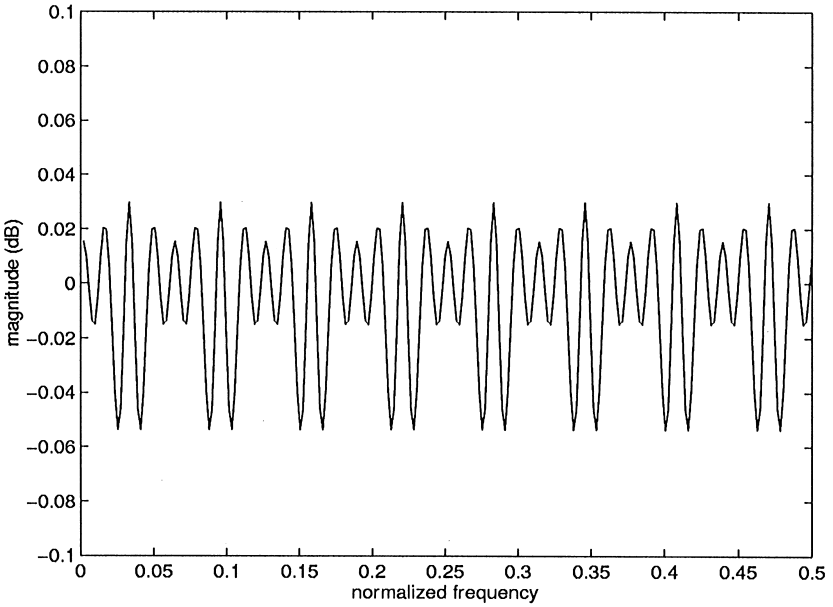

Fig. 9. Example 2: magnitude distortion function $M|T_0(e^{j\omega})|$.

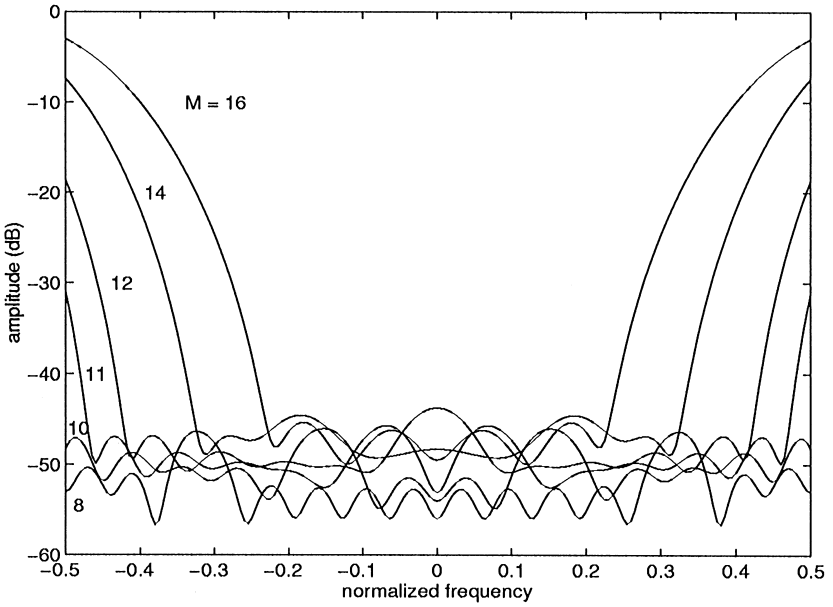

Fig. 10. Example 2: decimation aliasing $A(\omega)$ in subbands for different downsampling factors M.

F_s, into K subband components, respectively, $X_k(m)$ and $Y_k(m)$ $(k = 0,1,\ldots,K-1)$ with lower sampling rate $F'_s = F_s/M$. In each subband, $X_k(m)$ and $Y_k(m)$ are used as input and reference signals, respectively, to a transversal adaptive filter whose output (i.e. subband echo estimate) is subtracted from the reference $Y_k(m)$ to produce a residual signal $E_k(m)$. The subband residuals $E_k(m)$

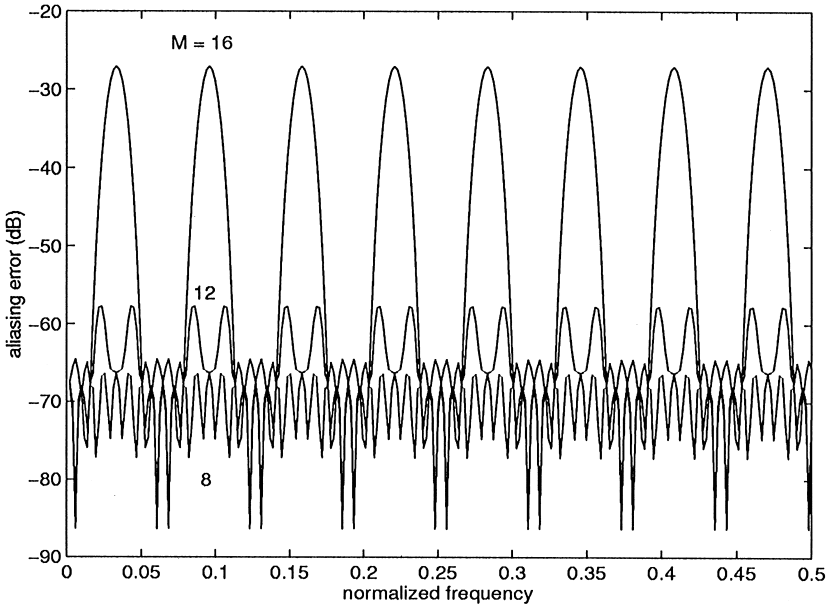

Fig. 11. Example 2: aliasing distortion $E(\omega)$ of the filter banks for different downsampling factors M.

$(k = 0, \ldots, K-1)$ are finally combined by the synthesis bank into a fullband output $e(n)$ at the rate F_s.[1]

This system was implemented on a TMS320C40 processor from Texas Instrument, a 32-bit floating point device operating at 50 MHz [16]. As our application focuses on voice communication over digital telephone networks, the sampling rate F_s is set to 8 kHz. For the subband processing, we use the modified DFT filter banks in Fig. 1 with $K = 16$ subbands, implemented efficiently via the WOA approach described in Section 4. The prototype filter $h(n)$ is designed as in Example 2, so that the results in Figs. 8–12 are all applicable here. Various decimation factors M are tried in the experiments. In each subband, transversal filters updated with the NLMS algorithm [2] are used for echo estimation; their lengths are adjusted independently so as to optimize system performance. Since the fullband signals $x(n)$ and $y(n)$ are real, there is no need to process the signals in subbands $k = 9$–15; their output is obtained through the symmetry relation $E_k(m) = E^*_{K-k}(m)$. Furthermore, subband $k = 0$ (0–250 Hz) and $k = 8$ (3.75–4 kHz) are deactivated, as they do not contain significant signal energy in toll-quality applications.

For the experiments, a communication link is established between two rooms, labeled A and B. A standard handset is used in room A (far-end); while a hands-free terminal, consisting of a small loudspeaker and an omnidirectional microphone, is used in room B (near-end), which is a small office. The duration of the acoustic impulse response between the loudspeaker and the microphone, as obtained through off-line measurements, is about 120 ms. The digital signals $x(n)$ and $y(n)$ are obtained through anti-aliasing filtering (cut-off at 3.5 kHz) followed by 16-bit A/D. Real speech, recorded speech and various synthetic signals are used in our experiments.

Here, we show results for white noise, but the conclusion remain generally valid for other types of signals. The lengths of the adaptive transversal filters in subband $k = 1$–7 are, respectively, set to 100,

[1] Other devices such as double-talk detector and echo suppressor, which are necessary for full-duplex operation of the subband AEC system but not directly relevant to this study, have been deactivated in our experiments.

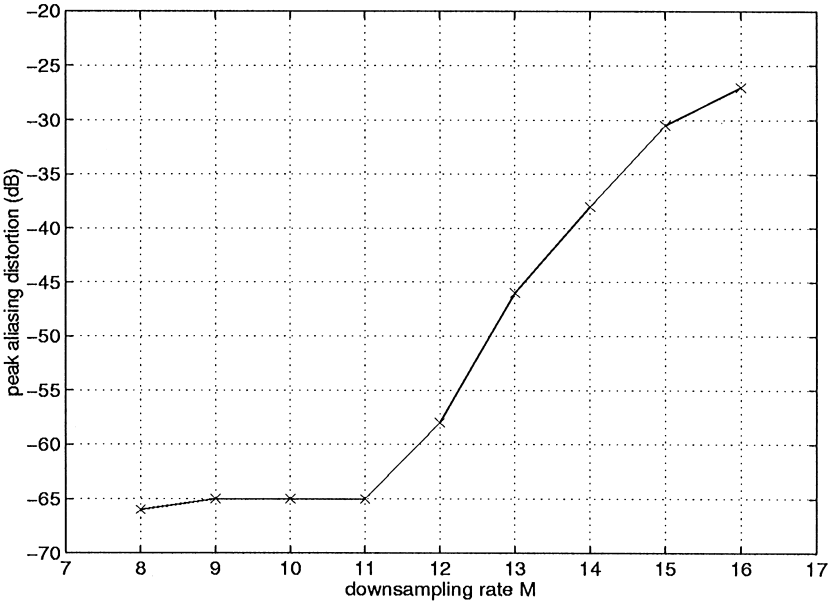

Fig. 12. Example 2: peak aliasing distortion for different downsampling factors M.

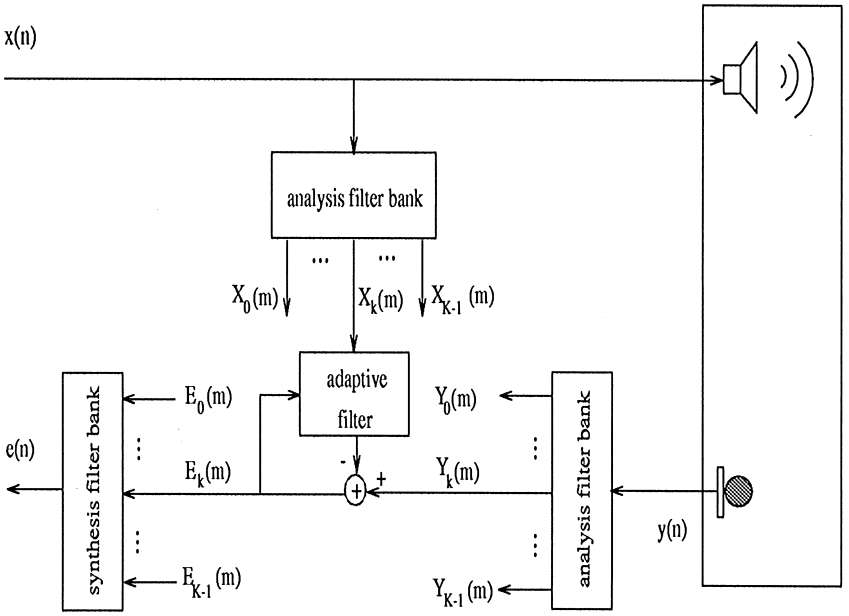

Fig. 13. Subband adaptive filtering structure.

100, 100, 90, 80, 70 and 60; the subband NLMS step size is set to 0.8. In Fig. 14, we show the initial convergence curves of the subband AEC system, i.e. short-term power of fullband output $e(n)$ versus discrete time n, for $M = 10$, 12 and 13. The results for $M = 10$ and 12 are quite similar: echo attenuation of 20 dB is obtained in about 0.6 s, while the residual echo level after convergence is around

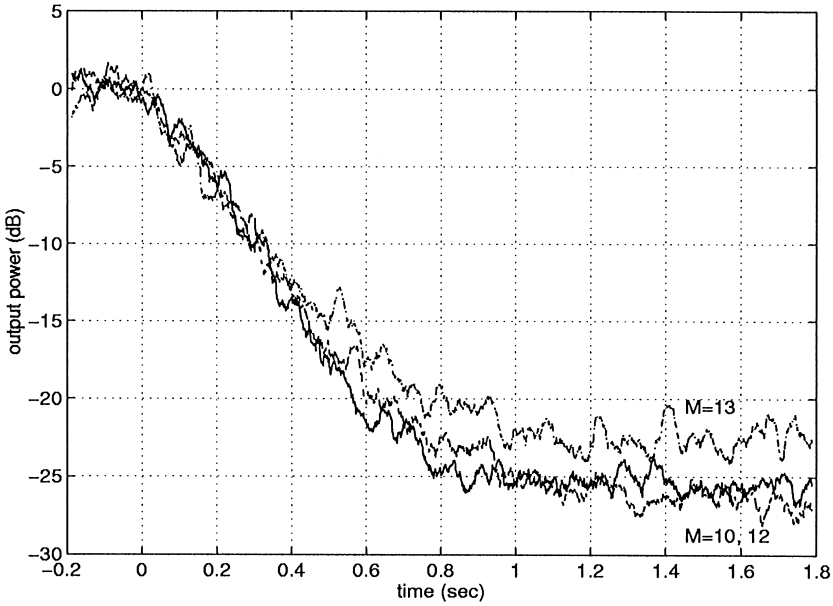

Fig. 14. Learning curves of subband AEC system for downsampling factors $M = 10$, 12 and 13 (white noise excitation).

-27 dB (due to background noise in room B and NLMS misadjustment). In the case $M = 13$, however, a larger residual level after convergence can be observed due to higher subband aliasing. From these results, we conclude that in this application, a decimation factor as high as $M = 12$ can be used without significantly affecting the cancellation performance of the subband AEC system.

6. Conclusion

In this work, a simple design technique for a modified uniform DFT filter bank is presented. The main features of the proposed filter bank include: (a) near-PR property under the oversampling scheme; (b) simple design procedure based on interpolation of a 2-channel QMF prototype; (c) efficient weighted-overlap-add realization. These characteristics are particularly interesting for engineering applications such as subband adaptive filtering. The effectiveness of the proposed method is demonstrated via design examples as well as experimental results in a real-time subband AEC application.

Finally, we point out that the complex filter bank proposed in this work can be easily extended to one with real subband signals by using the mapping found in [3] for the transformation of a complex DFT bank into a real one.

References

[1] P.L. Chu, Weaver SSB subband acoustic echo canceller, IEEE Workshop Applications on Signal Processing to Audio and Acoustics, October 1993, pp. 8–11.
[2] P.M. Clarkson, Optimal and Adaptive Signal Processing, CRC Press, Boca Raton, FL, 1993.
[3] R.E. Crochiere, L.R. Rabiner, Multirate Digital Signal Processing, Prentice-Hall, Englewood Cliffs, NJ, 1983.
[4] Z. Cvetković, M. Vetterli, Oversampling filter banks, IEEE Trans. Signal Process. 46 (May 1998) 1245–1255.
[5] B. Farhang-Boroujeny, Z. Wang, Adaptive filtering in subbands: design issues and experimental results for acoustic echo cancellation, Signal Processing 61 (1997) 213–223.
[6] S.L. Gay, R.J. Mammone, Fast converging subband acoustic echo cancellation using RAP on the WE@DSP14A, Proceedings of the ICASSP'90, April 1990, pp. 1141–1144.
[7] A. Gilloire, M. Vetterli, Adaptive filtering in subbands, Proceedings of the ICASSP'88, April 1988, pp. 1572–1575.

[8] A. Gilloire, M. Vetterli, Adaptive filtering in subbands with critical sampling: analysis, experiments, and application to acoustic echo cancellation, IEEE Trans. Signal Process. 40 (August 1992) 1862–1875.
[9] M. Harteneck, J.M. Páez-Borrallo, R.W. Stewart, An oversampled subband adaptive filter without cross adaptive filters, Signal Processing 64 (1998) 93–101.
[10] J.D. Johnston, A filter family designed for use in quadrature mirror filter banks, Proceedings of the ICASSP'80, April 1980, pp. 291–294.
[11] W. Kellermann, Analysis and design of multirate systems for cancellation of acoustical echoes, Proceedings of the ICASSP'88, April 1988, pp. 2570–2573.
[12] J. Kliewer, A. Mertins, Oversampled cosine-modulated filter banks with arbitrary system delay, IEEE Trans. Signal Process. 46 (April 1998) 941–955.
[13] R.D. Koilpillai, P.P. Vaidyanathan, Cosine-modulated FIR filter banks satisfying perfect reconstruction, IEEE Trans. Signal Process. 40 (April 1992) 770–783.
[14] T. Nagai, M. Ikehara, Design of oversampled perfect reconstruction FIR filter banks, Proceedings of the ISCAS'96, May 1996, pp. 328–332.
[15] H. Perez, F. Amano, S. Unagami, On the new structures of subband type echo canceler, IEICE Technical Report, SP89-119, February 1990.
[16] TMS320C4x User's Guide, Texas Instruments, 1993.
[17] P.P. Vaidyanathan, Multirate Systems and Filter Banks, Prentice-Hall, Englewood Cliffs, NJ, 1993.
[18] M. Vetterli, J. Kovacevic, Wavelet and Subband Coding, Prentice-Hall, Englewood Cliffs, NJ, 1995.